Partially coherent Gaussian–Schell model pulse beam propagation in slant atmospheric turbulence*

Li Ya-Qing(李亚清)[a], Wu Zhen-Sen(吴振森)[a]†, and Wang Ming-Jun(王明军)[b]

[a] School of Physics and Optoelectronic Engineering, Xidian University, Xi'an 710071, China
[b] School of Physics and Electronic Engineering, Xianyang Normal College, Xianyang 712000, China

(Received 23 October 2013; revised manuscript received 18 November 2013; published online 20 April 2014)

Based on the extended Huygens–Fresnel principle, a two-frequency, two-point cross-spectral density function of partially coherent Gaussian–Schell model pulse (GSMP) beam propagation in slant atmospheric turbulence is derived. Using the Markov approximation method and on the assumption that $(\omega_1 - \omega_2)/(\omega_1 + \omega_2) \leq 1$, the theory obtained is valid for turbulence of any strength and can be applied to narrow-band signals. The expressions for average beam intensity, the beam size, and the two-frequency complex degree of coherence of a GSMP beam are obtained. The numerical results are presented, and the effects of the frequency, initial pulse width, initial beam radius, zenith angle, and outer scales on the complex degree of coherence are discussed. This study provides a better understanding of the second-order statistics of a GSMP beam propagating through atmospheric turbulence in the space-frequency domain.

Keywords: atmospheric propagation, partial coherence, atmospheric turbulence

PACS: 42.25.Dd, 42.25.Kb, 42.68.Bz **DOI:** 10.1088/1674-1056/23/6/064216

1. Introduction

The problem of pulse signal propagation through atmospheric turbulence has received increasing attention in recent years. This interest is supported by the applications in areas such as ground-to-satellite, high-data-rate communication links, lidar operation, precise ranging as well as remote sensing. Mintzer[1] used the Born approximation to study the statistics of acoustic pulses in ocean turbulence. Subsequently, the signal distortion caused by the propagation of the pulse signal through random media was studied by Shirokova[2] and Knollman[3] using the Rytov approximation. Alimov and Erukhimov[4] proposed the statistical signal characteristics for the pulse signal through an inhomogeneous layer and reflection from the inhomogeneous layer using the phase screen method. Su and Plonus[5] discussed the statistical characteristics of the mean-square amplitude and phase fluctuations for optical pulse propagation through atmospheric turbulence by use of the Rytov method. As a follow-up to that study, Gardner and Plonus[6] used the Born approximation to study light pulse signal propagation in atmospheric turbulence. This approach has been used by a number of investigators to study the propagation of optical pulses in atmospheric turbulence.

The pulse propagation characteristics of a wave in a turbulent medium are determined by the two-frequency mutual coherence function (MCF). The two-frequency MCF is an important quantity by itself as it provides a measure of such pulse propagation characteristics as the instantaneous pulse intensity and the coherence bandwidth. In general, the two-frequency MCF provides a complete description of the second moment of a field. Using a different approach based on the two-frequency MCF, a number of authors[7–9] have investigated the propagation of pulses in a turbulent ionosphere and in an interplanetary medium. Most of these previous two-frequency MCF-based analyses have used the parabolic equation method, which is theoretically valid in all regimes of optical turbulence. Unfortunately, analytic solutions of the MCF by this method, using standard spectral models for refractive-index fluctuations, have been obtained only in the limiting case of a uniform plane wave.[9,10] Sreenivasiah and Ishimaru,[11] however, were successful in calculating the two-frequency MCF for a Gaussian pulse in a special case of a Gaussian atmospheric spectral model under the Markov approximation. Their solution is valid for wideband pulses and in the strong fluctuation regime.

Fante[12] used the extended Huygens–Fresnel principle to find the two-point, two-frequency MCF of an electromagnetic beam in a turbulent medium. Young *et al.*[13] developed an analytic expression for the two-frequency MCF of Gaussian beam pulses based on weak fluctuation theory and the modified von Karman spectrum for refractive-index fluctuations. In a weak turbulence, the Rytov approximation has been used to obtain an analytical expression for the MCF of Gaussian beam pulses through using the Kolmogorov spectrum of refractive-index fluctuations.[14] More recently, Antonio *et al.*[15,16] studied the long-term temporal broadening of a space–time Gaussian pulse propagating along a horizontal path through weak optical turbulence and depicted pulse distortion and broadening in atmospheric turbulence using a simple rate adaptive transmission technique. Chen *et al.*[17] studied the aver-

*Project supported by the National Natural Science Foundation of China (Grant Nos. 61172031 and 61271110).
†Corresponding author. E-mail: wuzhs@mail.xidian.edu.cn
© 2014 Chinese Physical Society and IOP Publishing Ltd

age spectral density and the spectral degree of coherence of a GSMP beam propagating in atmospheric turbulence based on the cross-spectral density function. Later, Chen *et al.*[18] derived an analytical formula for the turbulence-induced, temporal half-width of spherical-wave Gaussian (SWG) pulses propagating through either non-Kolmogorov or Kolmogorov turbulence under strong fluctuation conditions and the narrowband assumption. Furthermore, there are some researchers who have studied the propagation characteristics of other types of beams in atmospheric turbulence.[19–25]

Based on the extensive Huygens–Fresnel principle together with the paraxial approximation, we study the MCF of a partially coherent GSMP beam at a single frequency as well as at two frequencies under a modified von Karman turbulence spectrum in the slant path. In many applications, the exact shape of the pulse may not be needed. Rather, quantities such as the time delay, pulse broadening in the time-domain, the instantaneous intensity, and the complex degree of coherence of pulses in the frequency-domain caused by random scattering are of importance. Due to the complexity of the theory and the calculations involved in this study, we mainly concentrate on the instantaneous intensity, beam size, and spatial complex degree of coherence of the GSMP beam in the frequency-domain. An in-depth study related to the time delay and pulse broadening in the time-domain of the GSMP beam through atmospheric turbulence on the basis of the above theory will be undertaken in the future. In the frequency limiting case of $(\omega_1-\omega_2)/(\omega_1+\omega_2)\leq 1$, the proposed theory is theoretically valid at all levels of optical turbulence.

2. Analytical formulations

Supposing that a GSMP beam propagates from the source plane $z=0$ into the half-space $z>0$ (nearly parallel to the positive z axis), the MCF of a GSMP beam in the plane $z=0$ is given by[26]

$$\Gamma^{(0)}(\boldsymbol{r}_1,\boldsymbol{r}_2,t_1,t_2)=\Gamma_0\exp\left[-\Lambda(\boldsymbol{r}_1,\boldsymbol{r}_2)-\Xi(t_1,t_2)\right], \quad (1)$$

where $\boldsymbol{r}_1$ and $\boldsymbol{r}_2$ denote two position vectors in the plane $z=0$, Γ_0 is a constant, and

$$\Lambda(\boldsymbol{r}_1,\boldsymbol{r}_2)=\frac{r_1^2+r_2^2}{w_0^2}+\frac{|\boldsymbol{r}_1-\boldsymbol{r}_2|^2}{2\sigma_0^2}, \quad (2)$$

$$\Xi(t_1,t_2)=\frac{t_1^2+t_2^2}{2T_0^2}+\frac{(t_1-t_2)^2}{2T_c^2}+\mathrm{i}\omega_0(t_1-t_2), \quad (3)$$

where w_0 is the initial beam radius, σ_0 is the partially coherent length describing the partially coherent properties of the transmitter source, r_j is the modulus of $\boldsymbol{r}_j$ $(j=1,2)$, T_0 is the expectation value of the initial pulse width, T_c is the temporally coherent length, and ω_0 is the central angular frequency of the pulses. Using the Fourier transform, the cross-spectral density function of a GSMP beam in the source plane is given by[26]

$$W^{(0)}(\boldsymbol{r}_1,\boldsymbol{r}_2,\omega_1,\omega_2)=W_0\exp\left[-\Lambda(\boldsymbol{r}_1,\boldsymbol{r}_2)-\Xi(\omega_1,\omega_2)\right], \quad (4)$$

where ω_j $(j=1,2)$ is the angular frequency, $W_0=\Gamma_0T_0/(2\pi\Omega_0)$ is a coefficient independent of both position vectors and angular frequencies, $\Omega_0=\left(1/T_0^2+2/T_c^2\right)^{1/2}$ represents the spectral width, and

$$\Xi(\omega_1,\omega_2)=\frac{(\omega_1-\omega_0)^2+(\omega_2-\omega_0)^2}{2\Omega_0^2}+\frac{(\omega_1-\omega_2)^2}{2\Omega_c^2}, \quad (5)$$

with $\Omega_c=T_c\Omega_0/T_0$ representing the spectral coherence width. The cross-spectral density function of a GSMP beam in the source plane is written as

$$W^{(0)}(\boldsymbol{r}_1,\boldsymbol{r}_2,\omega_1,\omega_2)=W_0\exp\left[-\frac{r_1^2+r_2^2}{w_0^2}-\frac{(\boldsymbol{r}_1-\boldsymbol{r}_2)^2}{2\sigma_0^2}\right]\exp\left[-\Xi(\omega_1,\omega_2)\right]. \quad (6)$$

Assuming that any source fluctuations are statistically independent of the fluctuations in atmospheric turbulence and using the extended Huygens–Fresnel principle together with the paraxial approximation,[27] the cross-spectral density function of a GSMP beam in the half-space $z>0$ can be written as[12]

$$\begin{aligned}&W(\boldsymbol{\rho}_1,\boldsymbol{\rho}_2,\omega_1,\omega_2,z)\\&=\frac{\omega_1\omega_2}{(2\pi cz)^2}\int_{-\infty}^{\infty}\iiint \mathrm{d}^2r_1\,\mathrm{d}^2r_2W^{(0)}(\boldsymbol{r}_1,\boldsymbol{r}_2,\omega_1,\omega_2)\\&\times\exp\left\{\frac{\mathrm{i}(\omega_1-\omega_2)z}{c}+\frac{\mathrm{i}\omega_1}{2cz}(\boldsymbol{\rho}_1-\boldsymbol{r}_1)^2-\frac{\mathrm{i}\omega_2}{2cz}(\boldsymbol{\rho}_2-\boldsymbol{r}_2)^2\right\}\\&\times\left\langle\exp\left[\psi(\boldsymbol{r}_1,\boldsymbol{\rho}_1,\omega_1)+\psi^*(\boldsymbol{r}_2,\boldsymbol{\rho}_2,\omega_2)\right]\right\rangle,\end{aligned} \quad (7)$$

where $*$ represents the complex conjugate. Equation (7) includes the effects of turbulence and is valid for an arbitrary source coherence state. If it is assumed that the turbulence is statistically stationary and that the complex phase fluctuation ψ induced by the turbulence is a Gaussian random variable, it can be readily demonstrated that[28]

$$\left\langle\exp(\psi+\psi^*)\right\rangle=\exp\left[-\frac{1}{2}D_{12}(\boldsymbol{\rho}_1-\boldsymbol{\rho}_2,\boldsymbol{r}_1-\boldsymbol{r}_2)\right], \quad (8)$$

where

$$D_{12}(\boldsymbol{\rho}_1-\boldsymbol{\rho}_2,\boldsymbol{r}_1-\boldsymbol{r}_2)=\left\langle\left|\psi(\boldsymbol{\rho}_1,\boldsymbol{r}_1,\omega_1)-\psi(\boldsymbol{\rho}_2,\boldsymbol{r}_2,\omega_2)\right|^2\right\rangle. \quad (9)$$

Ishimaru[29] used the method of smooth perturbations to obtain a formal expression for D_{12} for isotropic turbulence that is expressed as

$$D_{12}(\boldsymbol{\rho}_1-\boldsymbol{\rho}_2,\boldsymbol{r}_1-\boldsymbol{r}_2)=(2\pi)^2\int_0^{\infty}k\,\mathrm{d}k\int_0^z\mathrm{d}z'\Phi_n(k,z')\left\{\frac{\omega_1^2+\omega_2^2}{c^2}\right.$$

$$-2\mathrm{J}_0(k\beta)\frac{\omega_1\omega_2}{c^2}\cos\left[\frac{z'c(z-z')}{2z}k^2\left(\frac{1}{\omega_1}-\frac{1}{\omega_2}\right)\right]\Bigg\}, \quad (10)$$

where

$$\beta=\left|\frac{z'}{z}(z-z')+\left(1-\frac{z'}{z}\right)(\boldsymbol{r}_1-\boldsymbol{r}_2)\right|. \quad (11)$$

The above term $\Phi_n(k,z')$ is the spectrum of the index-of-refraction fluctuations of the turbulence, $\mathrm{J}_0(x)$ is the zero-order Bessel function, and k is the optical wave number ($\omega = ck$). In deriving Eq. (10), it is implicitly assumed that the signal wavelength is smaller than the inner scale size of the turbulent eddies.

Because it has been assumed that ψ is a Gaussian random variable and because the method of smooth perturbations has been used to evaluate D_{12}, these results are strictly valid only in weak turbulence. However, in the limit when $\omega_1=\omega_2$, it has been found[30] that equations (8)–(10) are identical with the results obtained using the Markov approximation, an approach that is valid for turbulence of any strength. The valid range of Eqs. (8)–(10) for $\omega_1\neq\omega_2$ is uncertain, but it is expected that if $(\omega_1-\omega_2)/(\omega_1+\omega_2)\leq 1$, we can also safely use these results in turbulence of arbitrary strength.[12] We evaluate Eq. (10) for turbulence having a von Karman spectrum[12]

$$\Phi_n(k,z')=0.033C_n^2(z')\exp\left(-\frac{k^2l_0^2}{4\pi^2}\right)\left(k^2+\frac{1}{L_0^2}\right)^{-11/6}, \quad (12)$$

where $C_n^2(z')$ is the index-of-refraction structure constant[31] in the slant atmospheric turbulence, L_0 and l_0 are the outer and inner scale sizes of the turbulence, respectively. A diagram of the slant propagation is shown in Fig. 1.

In Fig. 1, θ is the path zenith angle, L is the slant length from the transmitter to the receiver, H is the vertical height of the receiver. h and z ($h\leq H$, $z\leq L$) are the vertical propagation height and the slant propagation distance of the beam, respectively, both of which are variables. Let $\xi=z'/z=h/H$ ($0<\xi<1$), the atmospheric structure constant $C_n^2(z')$ can be written as $C_n^2(\xi z)=C_n^2(\xi H/\cos\theta)$.

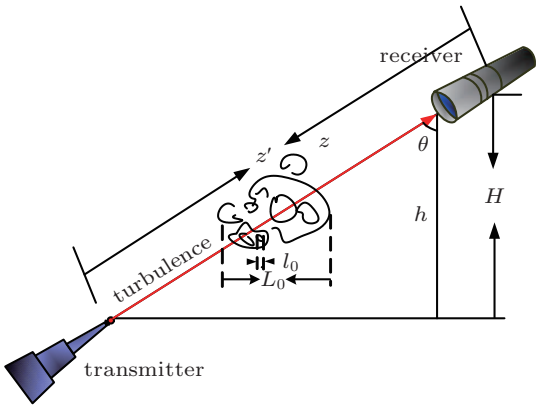


Fig. 1. (color online) Diagram of the laser beam propagation through atmospheric turbulence in the slant path.

If equation (12) is substituted into Eq. (10), we obtain

$$\begin{aligned}&D_{12}(\boldsymbol{\rho}_1-\boldsymbol{\rho}_2,\boldsymbol{r}_1-\boldsymbol{r}_2)\\&\approx 0.782L_0^{5/3}z\frac{(\omega_1-\omega_2)^2}{c^2}\int_0^1\mathrm{d}\xi C_n^2(\xi)\\&+8.69z\frac{\omega_1\omega_2}{c^2}\int_0^1\mathrm{d}\xi C_n^2(\xi)\\&\times\mathrm{Re}\left\{k_m^{-5/3}\left[{}_1\mathrm{F}_1\left(-\frac{5}{6},1,-\frac{k_m^2\beta^2}{4}\right)-1\right]\right\}, \quad (13)\end{aligned}$$

where ${}_1\mathrm{F}_1$ is the hypergeometric function, Re denotes the real part, and

$$k_m^2=\frac{1}{\left(\frac{l_0}{2\pi}\right)^2+\frac{\mathrm{i}zc\xi(1-\xi)}{2}\left(\frac{1}{\omega_1}-\frac{1}{\omega_2}\right)}. \quad (14)$$

Equation (13) can be simplified considerably under the following assumptions.[12]

Assuption 1 Either $|\boldsymbol{\rho}_1-\boldsymbol{\rho}_2|$ or $|\boldsymbol{r}_1-\boldsymbol{r}_2|$ is much greater than the inner scale size l_0, and is much smaller than the outer scale size L_0 of the turbulent eddies (reducing the diffraction and refraction effects of the turbulence on the beam);

Assuption 2 The quantity $\omega_\mathrm{d}\equiv\omega_1-\omega_2$ is sufficiently small that

$$\frac{\omega_\mathrm{d}}{\omega_\mathrm{c}}\ll\frac{2\omega_\mathrm{c}r_\mathrm{m}^2}{cz}, \quad (15)$$

where $\omega_\mathrm{c}\equiv(\omega_1+\omega_2)/2$ and $r_\mathrm{m}=\max(|\boldsymbol{\rho}_1-\boldsymbol{\rho}_2|,|\boldsymbol{r}_1-\boldsymbol{r}_2|)$.

When the aforementioned conditions are satisfied, equation (13) is reduced to

$$\begin{aligned}&D_{12}(\boldsymbol{\rho}_1-\boldsymbol{\rho}_2,\boldsymbol{r}_1-\boldsymbol{r}_2)\\&=0.782L_0^{5/3}z\frac{\omega_\mathrm{d}^2}{c^2}\int_0^1\mathrm{d}\xi C_n^2(\xi)+2.92\frac{\omega_1\omega_2}{c^2}z\\&\times\int_0^1\mathrm{d}\xi C_n^2(\xi)|\xi(\boldsymbol{\rho}_1-\boldsymbol{\rho}_2)+(1-\xi)(\boldsymbol{r}_1-\boldsymbol{r}_2)|^{5/3}. \quad (16)\end{aligned}$$

Note that equation (16) reduces to the conventional wave-structure function[32] when $\omega_1=\omega_2$, so that $\omega_\mathrm{d}=0$.

Substituting Eqs. (6), (8), and (16) into Eq. (7), and converting the center-of-mass coordinates $\boldsymbol{\rho}_\mathrm{c}$, $\boldsymbol{r}_\mathrm{c}$, ω_c and difference coordinates $\boldsymbol{\rho}_\mathrm{d}$, $\boldsymbol{r}_\mathrm{d}$, ω_d as follows:

$$\begin{aligned}&\boldsymbol{\rho}_\mathrm{c}=(\boldsymbol{\rho}_1+\boldsymbol{\rho}_2)/2,\quad \boldsymbol{\rho}_\mathrm{d}=\boldsymbol{\rho}_1-\boldsymbol{\rho}_2,\\&\boldsymbol{r}_\mathrm{c}=(\boldsymbol{r}_1+\boldsymbol{r}_2)/2,\quad \boldsymbol{r}_\mathrm{d}=\boldsymbol{r}_1-\boldsymbol{r}_2,\\&\omega_\mathrm{c}=(\omega_1+\omega_2)/2,\quad \omega_\mathrm{d}=\omega_1-\omega_2, \quad (17)\end{aligned}$$

equation (6) can be rewritten as

$$\begin{aligned}&W^{(0)}(\boldsymbol{r}_\mathrm{d},\boldsymbol{r}_\mathrm{c},\omega_\mathrm{d},\omega_\mathrm{c})\\&=W_0\exp\left[-\frac{2r_\mathrm{c}^2+r_\mathrm{d}^2/2}{w_0^2}-\frac{r_\mathrm{d}^2}{2\sigma_0^2}\right]\exp\left[-\Xi(\omega_\mathrm{d},\omega_\mathrm{c})\right], \quad (18)\end{aligned}$$

where

$$\Xi(\omega_\mathrm{d},\omega_\mathrm{c})=\frac{(\omega_\mathrm{c}-\omega_0)^2}{\Omega_0^2}+\left(\frac{1}{4\Omega_0^2}+\frac{1}{2\Omega_\mathrm{c}^2}\right)\omega_\mathrm{d}^2. \quad (19)$$

We can then rewrite Eq. (7) as

$$\begin{aligned} & W(\boldsymbol{\rho}_{\mathrm{d}}, \omega_{\mathrm{d}}, z) \\ = & C(\omega_{\mathrm{d}}) \int_{-\infty}^{\infty} \iiint \mathrm{d}^2 r_{\mathrm{d}} \mathrm{d}^2 r_{\mathrm{c}} W^{(0)}(\boldsymbol{r}_{\mathrm{d}}, \boldsymbol{r}_{\mathrm{c}}, \omega_{\mathrm{d}}, \omega_{\mathrm{c}}) \\ & \times \exp\left\{ \mathrm{i} \frac{\omega_{\mathrm{c}}}{cz} (\boldsymbol{\rho}_{\mathrm{c}} - \boldsymbol{r}_{\mathrm{c}}) \cdot (\boldsymbol{\rho}_{\mathrm{d}} - \boldsymbol{r}_{\mathrm{d}}) \right. \\ & + \mathrm{i} \frac{\omega_{\mathrm{d}}}{2cz} \left[(\boldsymbol{\rho}_{\mathrm{c}} - \boldsymbol{r}_{\mathrm{c}})^2 + \frac{1}{4} (\boldsymbol{\rho}_{\mathrm{d}} - \boldsymbol{r}_{\mathrm{d}})^2 \right] \\ & \left. - \eta(\boldsymbol{\rho}_{\mathrm{d}}, \boldsymbol{r}_{\mathrm{d}}, \omega_{\mathrm{d}}, \omega_{\mathrm{c}}) \right\}, \end{aligned} \tag{20}$$

where

$$C(\omega_{\mathrm{d}}) = \frac{(\omega_{\mathrm{c}}^2 - \omega_{\mathrm{d}}^2/4)}{(2\pi cz)^2} \exp\left(\mathrm{i}\omega_{\mathrm{d}} z/c - \alpha \omega_{\mathrm{d}}^2/c^2 \right), \tag{21}$$

$$\begin{aligned} & \eta(\boldsymbol{\rho}_{\mathrm{d}}, \boldsymbol{r}_{\mathrm{d}}, \omega_{\mathrm{d}}, \omega_{\mathrm{c}}) \\ = & 1.46 \left(\omega_{\mathrm{c}}^2 - \frac{\omega_{\mathrm{d}}^2}{4} \right) \frac{z}{c^2} \\ & \times \int_0^1 \mathrm{d}\xi C_n^2(\xi) |\boldsymbol{\rho}_{\mathrm{d}} \xi + \boldsymbol{r}_{\mathrm{d}}(1-\xi)|^{5/3}, \end{aligned} \tag{22}$$

$$\alpha = 0.391 L_0^{5/3} z \int_0^1 \mathrm{d}\xi C_n^2(\xi). \tag{23}$$

Approximating Eq. (22) by[12]

$$\begin{aligned} \eta = & \left(1.46\omega_{\mathrm{c}}^2 z/c^2\right)^{6/5} \\ & \times \int_0^1 \mathrm{d}\xi \left[C_n^2(\xi)\right]^{6/5} |\boldsymbol{\rho}_{\mathrm{d}} \xi + \boldsymbol{r}_{\mathrm{d}}(1-\xi)|^2, \end{aligned} \tag{24}$$

substituting Eqs. (18) and (24) into Eq. (20), we obtain

$$\begin{aligned} & W(\boldsymbol{\rho}_{\mathrm{d}}, \omega_{\mathrm{d}}, z) \\ = & W_0 C(\omega_{\mathrm{d}}) \exp\left[-\Xi(\omega_{\mathrm{d}}, \omega_{\mathrm{c}}) \right] \\ & \times \int_{-\infty}^{\infty} \iiint \mathrm{d}^2 r_{\mathrm{d}} \mathrm{d}^2 r_{\mathrm{c}} \exp\left[-\frac{2r_{\mathrm{c}}^2 + r_{\mathrm{d}}^2/2}{w_0^2} - \frac{r_{\mathrm{d}}^2}{2\sigma_0^2} \right] \\ & \times \exp\left\{ -l\rho_{\mathrm{d}}^2 - m\boldsymbol{\rho}_{\mathrm{d}} \cdot \boldsymbol{r}_{\mathrm{d}} - n r_{\mathrm{d}}^2 \right. \\ & + \mathrm{i} \frac{\omega_{\mathrm{c}}}{cz} (\boldsymbol{\rho}_{\mathrm{c}} - \boldsymbol{r}_{\mathrm{c}}) \cdot (\boldsymbol{\rho}_{\mathrm{d}} - \boldsymbol{r}_{\mathrm{d}}) \\ & \left. + \mathrm{i} \frac{\omega_{\mathrm{d}}}{2cz} \left[(\boldsymbol{\rho}_{\mathrm{c}} - \boldsymbol{r}_{\mathrm{c}})^2 + \frac{1}{4} (\boldsymbol{\rho}_{\mathrm{d}} - \boldsymbol{r}_{\mathrm{d}})^2 \right] \right\}, \end{aligned} \tag{25}$$

where $\Xi(\omega_{\mathrm{d}}, \omega_{\mathrm{c}})$ is given by Eq. (19).

By converting cylindrical coordinates into rectangular coordinates, we obtain the final expression for the cross-spectral density function of a GSMP beam in the half-space $z > 0$, which is valid for turbulence of any strength

$$\begin{aligned} & W(x_1, y_1, x_2, y_2, z) \\ = & \frac{\pi^2 \Delta}{dg} \exp\left[2l(x_1 x_2 + y_1 y_2) \right] \exp\left(\frac{p^2 + q^2}{d} + \frac{f^2 + h^2}{g} \right) \\ & \times \exp\left[\mathrm{i} \frac{\omega_{\mathrm{c}}}{2cz} \left(x_1^2 + y_1^2 - x_2^2 - y_2^2 \right) \right. \\ & \left. + \left(\mathrm{i} \frac{\omega_{\mathrm{d}}}{4cz} - l \right) \left(x_1^2 + y_1^2 + x_2^2 + y_2^2 \right) \right], \end{aligned} \tag{26}$$

where

$$\begin{aligned} \Delta &= W_0 C(\omega_{\mathrm{d}}) \exp\left[-\Xi(\omega_{\mathrm{d}}, \omega_{\mathrm{c}}) \right], \\ C(\omega_{\mathrm{d}}) &= \frac{(\omega_{\mathrm{c}}^2 - \omega_{\mathrm{d}}^2/4)}{(2\pi cz)^2} \exp\left(\mathrm{i}\omega_{\mathrm{d}} z/c - \alpha \omega_{\mathrm{d}}^2/c^2 \right), \\ b &= \frac{2}{w_0^2} - \mathrm{i} \frac{\omega_{\mathrm{d}}}{2cz}, \quad d = n + \frac{1}{2w_0^2} + \frac{1}{2\sigma_0^2} - \mathrm{i} \frac{\omega_{\mathrm{d}}}{8cz}, \\ g &= b + \frac{\omega_{\mathrm{c}}^2}{4c^2 z^2 d}, \\ \Xi(\omega_{\mathrm{d}}, \omega_{\mathrm{c}}) &= \frac{2\omega_{\mathrm{c}}^2 + 2\omega_0^2 + \omega_{\mathrm{d}}^2/2 - 4\omega_0 \omega_{\mathrm{c}}}{2\Omega_0^2} + \frac{\omega_{\mathrm{d}}^2}{2\Omega_{\mathrm{c}}^2}, \\ p &= -\mathrm{i} \frac{\omega_{\mathrm{c}}}{4cz} (x_1 + x_2) - \left(\mathrm{i} \frac{\omega_{\mathrm{d}}}{8cz} + \frac{m}{2} \right) (x_1 - x_2), \\ q &= -\mathrm{i} \frac{\omega_{\mathrm{c}}}{4cz} (y_1 + y_2) - \left(\mathrm{i} \frac{\omega_{\mathrm{d}}}{8cz} + \frac{m}{2} \right) (y_1 - y_2), \\ f &= \mathrm{i} \frac{\omega_{\mathrm{c}} p}{2czd} - \mathrm{i} \frac{\omega_{\mathrm{d}}}{4cz} (x_1 + x_2) - \mathrm{i} \frac{\omega_{\mathrm{c}}}{2cz} (x_1 - x_2), \\ h &= \mathrm{i} \frac{\omega_{\mathrm{c}} q}{2czd} - \mathrm{i} \frac{\omega_{\mathrm{d}}}{4cz} (y_1 + y_2) - \mathrm{i} \frac{\omega_{\mathrm{c}}}{2cz} (y_1 - y_2), \\ l &= \left(1.46\omega_{\mathrm{c}}^2 z/c^2\right)^{6/5} \int_0^1 \xi^2 \left[C_n^2(\xi)\right]^{6/5} \mathrm{d}\xi, \\ m &= 2\left(1.46\omega_{\mathrm{c}}^2 z/c^2\right)^{6/5} \int_0^1 \xi(1-\xi) \left[C_n^2(\xi)\right]^{6/5} \mathrm{d}\xi, \\ n &= \left(1.46\omega_{\mathrm{c}}^2 z/c^2\right)^{6/5} \int_0^1 (1-\xi)^2 \left[C_n^2(\xi)\right]^{6/5} \mathrm{d}\xi. \end{aligned}$$

2.1. Average beam intensity and beam size

Let $\rho_1 = \rho_2 = \rho$, $\omega_1 = \omega_2 = \omega$, then average beam intensity will be obtained from Eq. (26) as

$$\begin{aligned} & I(\boldsymbol{\rho}, \omega, z) \\ = & W(\boldsymbol{\rho}, \boldsymbol{\rho}, \omega, \omega, z) \\ = & \frac{W_0}{\chi(\omega, z)} \exp\left[-\frac{2\rho^2}{w_0^2 \cdot \chi(\omega, z)} \right] \exp\left[-\frac{(\omega - \omega_0)^2}{\Omega_0^2} \right], \end{aligned} \tag{27}$$

where

$$\begin{aligned} \chi(\omega, z) &= 1 + \frac{4c^2 z^2}{w_0^2 \omega^2} \left(2n + \frac{1}{w_0^2} + \frac{1}{\sigma_0^2} \right), \\ n &= \left(1.46\omega^2 z/c^2\right)^{6/5} \int_0^1 (1-\xi)^2 \left[C_n^2(\xi)\right]^{6/5} \mathrm{d}\xi. \end{aligned} \tag{28}$$

Now, we consider how the random medium affects the spot size of the beam. The radius w_{c} of the beam spot is defined as[11]

$$I(\rho = W_{\mathrm{c}}, \rho_{\mathrm{d}} = 0, z) / I(\rho = \rho_{\mathrm{d}} = 0, z) = \exp(-2). \tag{29}$$

The equation for the beam size w_{c} of a collimated beam is obtained as

$$w_{\mathrm{c}} = w_0 \chi(\omega, z)^{1/2}, \tag{30}$$

where w_0 is the initial beam radius and $\chi(\omega, z)$ is given by Eq. (28).

2.2. Pulse propagation

2.2.1. Two-frequency, single-point complex degree of coherence

Let $\rho_1 = \rho_2 = \rho$, $\omega_1 \neq \omega_2$, then equation (26) will be expressed as

$$\begin{aligned} & W(\rho,\rho,\omega_1,\omega_2,z) \\ &= \frac{\pi^2\Delta}{dg}\exp\left\{\left[\frac{1}{4c^2z^2dg}\left(\frac{\omega_c^4}{4c^2z^2d}-g\omega_c^2\right.\right.\right. \\ &\quad \left.\left.\left.-\mathrm{d}\omega_d^2-\mathrm{i}\frac{\omega_c^2\omega_d}{cz}\right)+\mathrm{i}\frac{\omega_d}{2cz}\right]\rho^2\right\}, \end{aligned} \tag{31}$$

where

$$\Delta = W_0 C(\omega_d)\exp\left[-\frac{(\omega_c-\omega_0)^2}{\Omega_0^2}-\left(\frac{1}{4\Omega_0^2}+\frac{1}{2\Omega_c^2}\right)\omega_d^2\right],$$

$$C(\omega_d) = \frac{(\omega_c^2-\omega_d^2/4)}{(2\pi zc)^2}\exp\left(\mathrm{i}\omega_d z/c-\alpha\omega_d^2/c^2\right),$$

$$d = n+\frac{1}{2w_0^2}+\frac{1}{2\sigma_0^2}-\mathrm{i}\frac{\omega_d}{8cz},$$

$$g = \frac{2}{w_0^2}+\frac{\omega_c^2}{4c^2z^2d}-\mathrm{i}\frac{\omega_d}{2cz}.$$

The two-frequency, single-point complex degree of coherence in the z plane is expressed as[13]

$$\begin{aligned} & \gamma(\rho,\rho,\omega_1,\omega_2,z) \\ &= \frac{W(\rho,\rho,\omega_1,\omega_2,z)}{W^{1/2}(\rho,\rho,\omega_1,\omega_1,z)W^{1/2}(\rho,\rho,\omega_2,\omega_2,z)}, \end{aligned} \tag{32}$$

where $W(\rho,\rho,\omega_1,\omega_2,z)$ and $W(\rho,\rho,\omega_j,\omega_j,z)$, $j=1,2$ are given by Eqs. (31) and (27), respectively.

2.2.2. Single-frequency, two-point complex degree of coherence

Let $\rho_1 \neq \rho_2$, $\omega_1 = \omega_2 = \omega$, then equation (26) will be written as

$$\begin{aligned} & W(\rho_1,\rho_2,\omega,\omega,z) \\ &= W(x_1,y_1,x_2,y_2,z) \\ &= \frac{\pi^2\Delta}{dg}\exp\left[2l(x_1x_2+y_1y_2)\right]\exp\left(\frac{p^2+q^2}{d}+\frac{f^2+h^2}{g}\right) \\ &\quad \times\exp\left[\mathrm{i}\frac{\omega}{2cz}\left(x_1^2+y_1^2-x_2^2-y_2^2\right)\right. \\ &\quad \left.-l\left(x_1^2+y_1^2+x_2^2+y_2^2\right)\right], \end{aligned} \tag{33}$$

where

$$\Delta = W_0\left(\frac{\omega}{2\pi cz}\right)^2\exp\left[-\frac{(\omega-\omega_0)^2}{\Omega_0^2}\right],$$

$$d = n+\frac{1}{2w_0^2}+\frac{1}{2\sigma_0^2},\quad g = \frac{2}{w_0^2}+\frac{\omega^2}{4c^2z^2d},$$

$$p = -\mathrm{i}\frac{\omega}{4cz}(x_1+x_2)-\frac{m}{2}(x_1-x_2),$$

$$q = -\mathrm{i}\frac{\omega}{4cz}(y_1+y_2)-\frac{m}{2}(y_1-y_2),$$

$$f = \mathrm{i}\frac{\omega p}{2czd}-\mathrm{i}\frac{\omega}{2cz}(x_1-x_2),$$

$$h = \mathrm{i}\frac{\omega q}{2czd}-\mathrm{i}\frac{\omega}{2cz}(y_1-y_2),$$

$$l = \left(1.46\omega^2z/c^2\right)^{6/5}\int_0^1\xi^2\left[C_n^2(\xi)\right]^{6/5}\mathrm{d}\xi,$$

$$m = 2\left(1.46\omega^2z/c^2\right)^{6/5}\int_0^1\xi(1-\xi)\left[C_n^2(\xi)\right]^{6/5}\mathrm{d}\xi,$$

$$n = \left(1.46\omega^2z/c^2\right)^{6/5}\int_0^1(1-\xi)^2\left[C_n^2(\xi)\right]^{6/5}\mathrm{d}\xi.$$

The single-frequency, two-point complex degree of coherence is expressed as

$$\begin{aligned} & \gamma(\rho_1,\rho_2,\omega,\omega,z) \\ &= \frac{W(\rho_1,\rho_2,\omega,\omega,z)}{W^{1/2}(\rho_1,\rho_1,\omega,\omega,z)W^{1/2}(\rho_2,\rho_2,\omega,\omega,z)}, \end{aligned} \tag{34}$$

where $W(\rho_1,\rho_2,\omega,\omega,z)$ and $W(\rho_j,\rho_j,\omega,\omega,z)$, $j=1,2$ are given by Eqs. (33) and (27), respectively.

2.2.3. Two-frequency, two-point complex degree of coherence

Using Eq. (26), we obtain the two-frequency, two-point complex degree of coherence as follows:

$$\begin{aligned} & \gamma(\rho_1,\rho_2,\omega_1,\omega_2,z) \\ &= \frac{W(\rho_1,\rho_2,\omega_1,\omega_2,z)}{W^{1/2}(\rho_1,\rho_1,\omega_1,\omega_1,z)W^{1/2}(\rho_2,\rho_2,\omega_2,\omega_2,z)}, \end{aligned} \tag{35}$$

where $W(\rho_1,\rho_2,\omega_1,\omega_2,z)$ and $W(\rho_j,\rho_j,\omega_j,\omega_j,z)$, $j=1,2$ are given by Eqs. (26) and (27), respectively.

3. Numerical results and analyses

We consider a GSMP beam, of which the central wavelength λ_0, corresponding to the central angular frequency $\omega_0 = 1.2\times10^6$ GHz ($\omega_1 = 1.198\times10^6$ GHz, $\omega_2 = 1.202\times10^6$ GHz), is 1.55 μm, and the expectation value of the initial pulse width T_0 is 200 fs (when $T_0 > 20$ fs, the signal is narrow band, 1 fs = 1×10^{-15} s). Note that the angular frequency ω is related to wavelength λ by $\omega = 2\pi c/\lambda$, the numerical results in Figs. 2–6 are all based on taking values of $H = 500$ m, $\theta = 60^\circ$, and $L_0 = 1$ m. If $T_c = \infty$ (when $T_c = \infty$ and $\sigma_0 = \infty$, the beam is fully coherent), the spectral width $\Omega_0 = 5\times10^3$ GHz, and, for the case of $T_c = 100$ fs, the spectral width $\Omega_0 = 1.5\times10^4$ GHz. These parameters are chosen to meet the conditions of $(\omega_1-\omega_2)/(\omega_1+\omega_2) \leq 1$ and $\omega_d/\omega_c \ll 2\omega_c r_m^2/cz$.

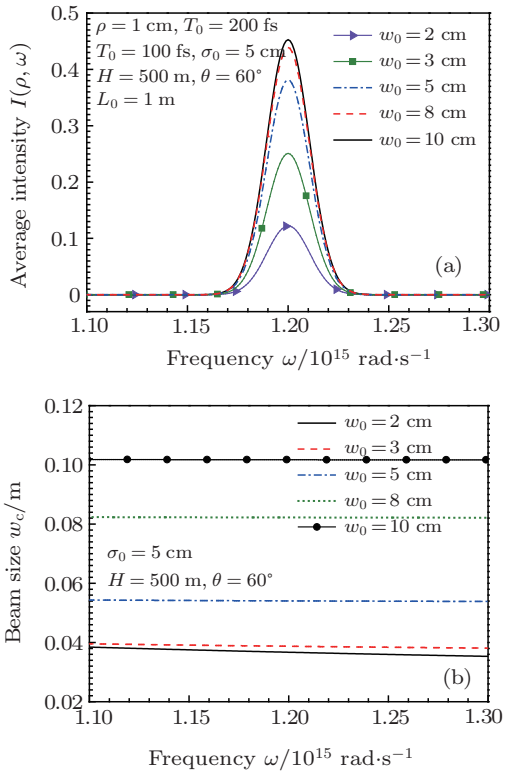


Fig. 2. (color online) Variations of (a) average intensity and (b) beam size with frequency for different initial beam radii.

As shown in Fig. 2(a), in the frequency range near the central angular frequency (1.16×10^6 GHz$< \omega < 1.24 \times 10^6$ GHz), the average intensity is not equal to zero but obtains its maximum value near the central angular frequency. Within this frequency band, the average intensity increases with increasing initial beam radius. Figure 2(b) shows that the variation of the beam size with changing frequency is not obvious when the beam propagates through atmospheric turbulence, i.e., the magnitude of the frequency has a small effect on the beam size in atmospheric turbulence. Finally, a larger initial beam radius indicates a greater beam size.

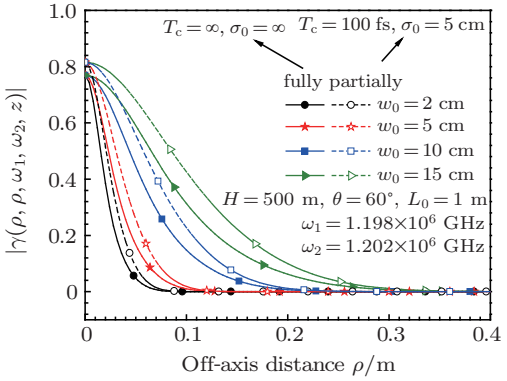


Fig. 3. (color online) Two-frequency, single-point complex degrees of coherence of beams versus the off-axis distance ρ for different initial beam radii.

Figure 3 shows the comparisons between the two-frequency, single-point complex degree of coherence of the partially coherent GSMP beam and that of the fully coherent Gaussian pulse beam for different initial beam radii. We note that as we move away from the beam axis, the complex degree of coherence decreases and the value is close to be zero when the off-axis distance reaches a certain value (for the partially coherent GSMP beam with $w_0 = 5$ cm, $|\gamma| \to 0$ when $\rho = 11.2$ cm). We notice that the off-axis distance corresponding to the complex degree of coherence close to zero shifts to a larger value as the initial beam radius increases. The complex degree of coherence of the partially coherent GSMP beam is larger than that of the fully coherent Gaussian beam, and a larger initial beam radius indicates a greater complex degree of coherence.

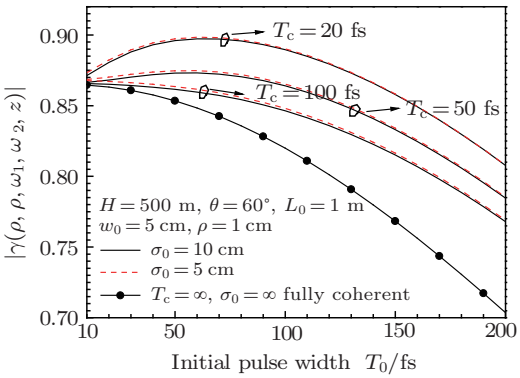


Fig. 4. (color online) Two-frequency, single-point complex degrees of coherence of beams versus the initial pulse width T_0 for different values of temporally coherent length T_c and partially coherent length σ_0.

Figure 4 shows that the values of $|\gamma(\rho, \rho, \omega_1, \omega_2, z)|$ versus T_0 for $\sigma_0 = 10$ cm and $\sigma_0 = 5$ cm are very close together for beams having identical values of T_c, but the values of $|\gamma|$ for beams having different values of T_c vary considerably. i.e., the temporally coherent length imposes a more maximal effect on $|\gamma(\rho, \rho, \omega_1, \omega_2, z)|$ than on that of the partially coherent length, and the smaller the temporally coherent length, the larger the complex degree of coherence is.

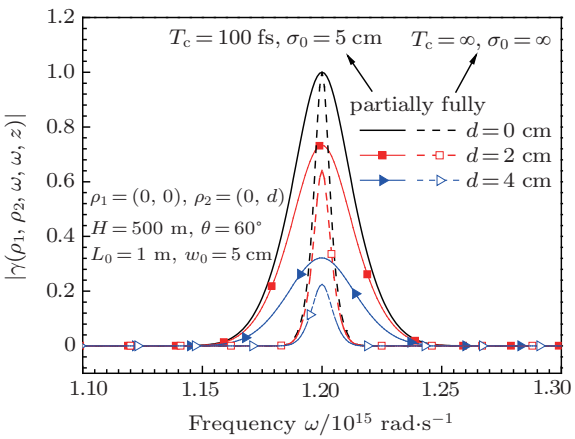


Fig. 5. (color online) Single-frequency, two-point complex degrees of coherence of beams versus frequency ω for different values of distance d between the two points.

We use Eq. (34) to compute $|\gamma(\rho_1,\rho_2,\omega,\omega,z)|$. The results are shown in Fig. 5. In a range of frequency near the central angular frequency ω_0, the single-frequency, two-point complex degree of coherence is not close to zero. However, the value of $|\gamma|$ tends towards zero when the frequency varies outside this range and the range of the fully coherent Gaussian beam is small compared with that of the partially coherent GSM beam. Furthermore, $|\gamma|$ at the central angular frequency reaches its maximum value. The complex degree of coherence of a partially coherent beam is larger than that of a fully coherent beam with the same value of d. It can be seen that at the central angular frequency, $|\gamma(\rho_1,\rho_2,\omega,\omega,z)|=1$ if a spatially partially coherent pulsed beam ($T_c\neq\infty,\sigma_0\neq\infty$) propagates through atmospheric turbulence when $d=0$, this result agrees with what one might expect (in this sense, the use of a partially coherent beam is better than that of a fully coherent beam). We find that $|\gamma|$ varies more rapidly with ω as the value of d decreases. The value of $|\gamma|$ decreases with increasing distances between the two points. Figure 5 shows that no matter whether spatially partial coherence of the source or atmospheric turbulence is present, the complex degree of coherence is smaller for a GSMP beam at a higher frequency than at a lower frequency when $\omega>\omega_0$, which is opposite to the result when $\omega<\omega_0$. This is inconsistent with the results of Fig. 1 in Ref. [17], in which it was generally considered that in the presence of spatially partial coherence of the source and (or) atmospheric turbulence, the degree of transverse spatial coherence in an observation plane $z>0$ was slightly smaller for a GSMP beam at a higher frequency than at a lower frequency. The degree of coherence for a GSMP beam is dependent on the frequency, but the central angular frequency ω_0 is the critical point.

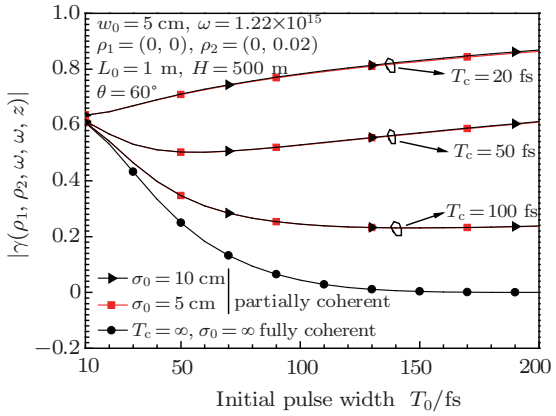


Fig. 6. (color online) Single-frequency, two-point complex degrees of coherence of beams versus the initial pulse width T_0 for different values of temporally coherent length T_c and partially coherent length σ_0.

As shown in Fig. 6, when T_0 changes from 10 fs to 200 fs, there is nearly no change in $|\gamma|$ with identical values of T_c for different values of σ_0. The substantial variation in $|\gamma|$ observed for different values of T_c, for constant values of σ_0, shows that the effect of T_c on the complex degree of coherence is much greater than that of σ_0. This result is consistent with that in Fig. 4, but the values of $|\gamma|$ versus T_0 curves are different for the cases of the single-frequency, two-point complex degree of coherence and the two-frequency, single-point one.

We take that $\rho_1=(0.01,0.03)$, $\rho_2=(0.01,0.06)$, $\omega_0=1.2\times10^6$ GHz ($\omega_1=1.198\times10^6$ GHz, $\omega_2=1.202\times10^6$ GHz).

Figure 7(a) shows that the two-frequency, two-point complex degree of coherence decreases with increasing zenith angle θ, the complex degree of coherence approaches to zero when the zenith angle is close to 90° (representing horizontal propagation). As the initial beam radius increases, the value of $|\gamma|$ decreases. While this effect is significant for $w_0=5$ cm, the curves of $|\gamma|$ versus θ for $w_0>5$ cm are very close together when $\theta\leq45°$. This is to be expected since $|\gamma|$ does not depend on w_0 when $w_0>5$ cm and $\theta\leq45°$. Figure 7(b) shows that if the value of zenith angle is a fixed one, the two-frequency, two-point complex degree of coherence decreases as the receiver height increases, and the value of $|\gamma|$ decreases with the increasing magnitude of the turbulence outer-scale, while the larger the outer-scale, the greater the effect on the complex degree of coherence is.

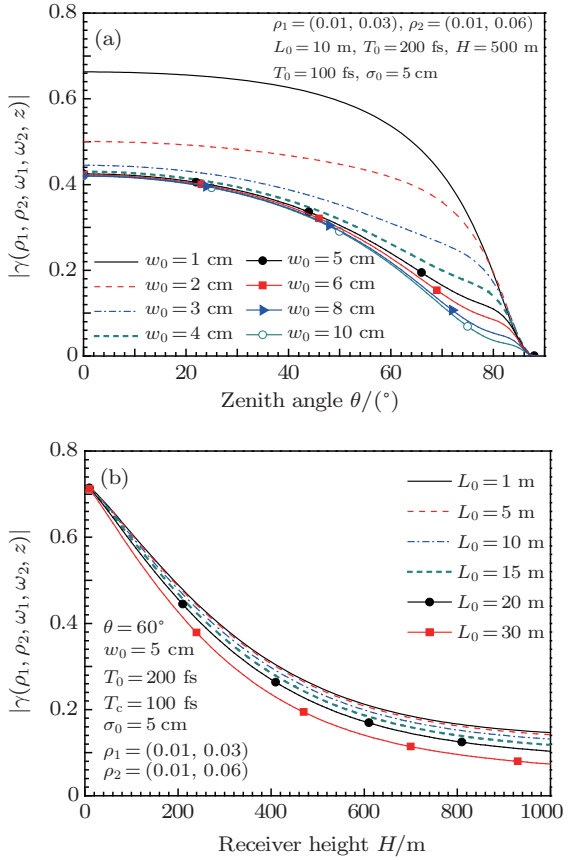


Fig. 7. (color online) Two-frequency, two-point complex degrees of coherence versus (a) zenith angle for different initial beam radii, and (b) receiver height for different outer scales.

Figure 8(a) shows that there is little change in the variation of $|\gamma(\rho_1,\rho_2,\omega_1,\omega_2,z)|$ with T_0 for the fully coherent beam. The partially coherent length exerts a greater effect on the complex degree of coherence than the temporally coherent length, which is contrary to the results shown in Figs. 4 and 6. Figure 8(b) shows that the variation of $|\gamma|$ with T_0 is not obvious for different distances between the two points, and that the values of $|\gamma|$ change more gently with changing values of T_0 as the distance between the two points increases. The size of d has a large influence on the complex degree of coherence, and the complex degree of coherence decreases with increasing distance between the two points.

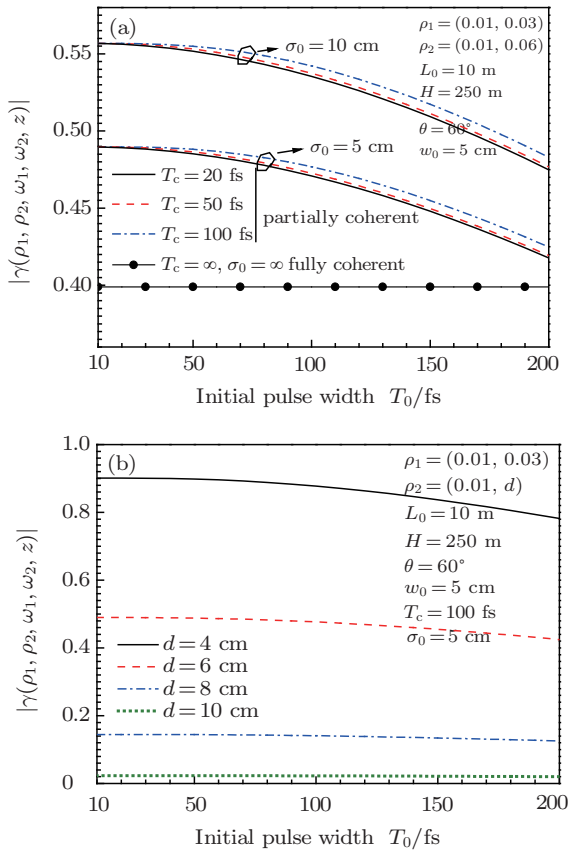


Fig. 8. (color online) Two-frequency, two-point complex degrees of coherence versus initial pulse width T_0 for different values of (a) temporally coherent length T_c and partially coherent length σ_0, and (b) distance d between the two points.

4. Conclusions

In this study, novel analytical expressions for the two-frequency, two-point cross-spectral density function of a GSMP beam propagating through atmospheric turbulence are derived using the extended Huygens–Fresnel principle and the quadratic approximation of the random phase structure function. Using the Markov approximation method and on the assumption that $(\omega_1-\omega_2)/(\omega_1+\omega_2)\leq 1$, the results obtained are valid for turbulence of any strength and can be applied to narrow-band signals. From the cross-spectral density function, the expressions for the average beam intensity, beam size, and the two-frequency degree of coherence of a GSMP beam are obtained. It is shown that the average intensity and the complex degree of coherence reach a maximum at the central angular frequency and that the magnitude of the frequency has a small influence on beam size in atmospheric turbulence. For the variations of the two-frequency, single-point and the single-frequency, two-point complex degree of coherence with the initial pulse width T_0, the temporally coherent length exerts a greater effect on the complex degree of coherence than the partially coherent length, which is contrary to the results derived for the two-frequency, two-point complex degree of coherence. The value of the single-frequency, two-point and the two-frequency, two-point complex degree of coherence decreases with increasing distance between the two points. The two-frequency, two-point complex degree of coherence decreases with increasing zenith angle and receiver height, and decreases as the turbulence outer-scale increases. The complex degree of coherence of the partially coherent GSM beam is larger than that of the fully coherent Gaussian beam, and a larger initial beam radius indicates a greater complex degree of coherence.

The research work outlined in this report provides a better understanding of the second-order statistics of a GSMP beam propagating through atmospheric turbulence in the space-frequency domain. Our results are useful for applications involving spatially and spectrally partially coherent pulsed beams. It should be mentioned that our analytical expressions for the cross-spectral density function also provide a basis for the numerical study of the propagation characteristics of a GSMP beam through atmospheric turbulence in the space-time domain.

References

[1] Mintzer D 1953 *J. Acoust. Soc. Am.* **25** 922
[2] Shirokova T A 1963 *Sov. Phy. Acoust.* **9** 78
[3] Knollman G C 1965 *J. Appl. Phys.* **36** 3704
[4] Alimov V A and Erukhimov L M 1968 *Radiophys. Quantum Electron.* **11** 268
[5] Su H H and Plonus M A 1971 *J. Opt. Soc. Am.* **61** 256
[6] Gardner C S and Plonus M A 1974 *J. Opt. Soc. Am.* **64** 68
[7] Erukhimov L M, Zarnitsyna I G A and Kirsh P I 1973 *Radiophys. Quantum Electron.* **16** 436
[8] Liu C H, Wernik A W and Yeh K C 1974 *IEEE Trans. Anten. Propag.* **22** 624
[9] Lee L C and Jokipii J R 1975 *Astrophys. J.* **201** 532
[10] Sreenivasiah I, Ishimaru A and Hong S T 1976 *Radio Sci.* **11** 775
[11] Sreenivasiah I and Ishimaru A 1979 *Appl. Opt.* **18** 1613
[12] Fante R L 1981 *J. Opt. Soc. Am.* **71** 1446
[13] Young C Y, Ishimaru A and Andrews L C 1996 *Appl. Opt.* **35** 6522
[14] Young C Y, Andrews L C and Ishimaru A 1998 *Appl. Opt.* **37** 7655

[15] Jurado-Navas A, Garrido-Balsells J M, Castillo-Vázquez M and Puerta-Notario A 2009 *Opt. Lett.* **34** 3662
[16] Antonio J N, María G-B José, Miguel C-Vázquez and Antonio P N 2010 *Opt. Express* **18** 17346
[17] Chen C Y, Yang H M, Lou Y and Tong S F 2011 *Opt. Express* **19** 15196
[18] Chen C Y, Yang H M, Lou Y, Tong S F and Liu R C 2012 *Opt. Express* **20** 7749
[19] Zhang M, Wu Z S, Zhang Y D and Yang T G 2001 *Acta Phys. Sin.* **50** 1052 (in Chinese)
[20] Wang T and Pu J X 2007 *Acta Phys. Sin.* **56** 6754 (in Chinese)
[21] Li J H, Yang A L and Lü B D 2009 *Acta Phys. Sin.* **58** 674 (in Chinese)
[22] Lü B D, Li J H and Zhang H R 2010 *Chin. Phys. B* **19** 099201
[23] Ji X L 2010 *Acta Phys. Sin.* **59** 3953 (in Chinese)
[24] Li Y Q and Wu Z S 2012 *Chin. Phys. B* **21** 054203
[25] Fang G J and Pu J X 2012 *Chin. Phys. B* **21** 084203
[26] Lajunen H, Vahimaa P and Tervo J 2005 *J. Opt. Soc. Am. A* **22** 1536
[27] Andrews L C and Phillips R L 2005 *Laser Beam Propagation Through Random Media* (Washington: SPIE Press Bellingham) Chaps. 4 and 5
[28] Fante R 1980 *Proc. IEEE* **68** 1424
[29] Ishimaru A 1972 *IEEE Trans. Anten. Propag.* **20** 10
[30] Fante R and Poirier J 1973 *Appl. Opt.* **12** 2247
[31] ITU-R Document 3J/31-E 2001 *Radio Communication Study Group Meeting*, Budapest, Hungary, **206** p. 277
[32] Tatarskii V 1971 *The Effect of the Turbulent Atmosphere on Wave Propagation* (Springfield: Israel Program for Scientific Translations) p. 148